

ON THE INTERPRETATION OF MELT QUALITY ASSESSMENT OF A356 ALUMINUM ALLOY BY THE REDUCED PRESSURE TEST: THE BIFILM INDEX AND ITS PHYSICAL MEANING

Muhammet Uludağ

Faculty of Engineering, Bursa Technical University, Bursa, Turkey

Remzi Çetin

Faculty of Engineering, Karatay University, Konya, Turkey

Derya Dişpınar

Faculty of Engineering, Istanbul University, Istanbul, Turkey

Murat Tiryakioğlu

School of Engineering, University of North Florida, Jacksonville, FL, USA

Copyright © 2018 American Foundry Society
<https://doi.org/10.1007/s40962-018-0217-4>

Abstract

The oxide layer on liquid aluminum serves as a protective property to prevent the alloy from further oxidation. However, it has the potential to be a source of porosity when entrained into the bulk of the liquid. For this reason, oxides entrained into aluminum castings have been shown to degrade casting quality. In the current study, the effectiveness of the reduced pressure test in assessing the quality of A356 alloy melts has been investigated under various conditions obtained by changing six different melt parameters. Several metrics, including average pore size,

number density of pores, bifilm index, have been used to measure melt quality. Results have shown that the bifilm index provides reliable measurements of melt quality. Moreover, the bifilm index has been found to have a physical meaning, volume fraction of pores, especially when bifilm index is higher than 50 mm.

Keywords: A356, casting, quality, bifilm index, RPT, porosity, modification, grain refinement

Introduction

It is well known that a high-quality casting cannot be produced without a high-quality melt. Therefore, a significant effort has been made to not only determine melt treatments that improve melt quality, but also develop measurement techniques and metrics that can be used reliably to assess melt quality. Foundry engineers need metrics and reliable techniques to validate whether the melt treatments, such as grain refining and degassing, have indeed improved the quality of the melt. This need has led to the development of many early techniques¹⁻⁶ as well as those more recent ones⁷⁻¹⁰ which usually rely on the measurement of hydrogen by probes where the activity of hydrogen in the melt is analyzed by Sieverts law. These

recent techniques, however, are usually regarded as complex and expensive. Therefore, the most common technique in use remains to be the reduced pressure test (RPT), in which a sample taken from the melt is allowed to solidify under reduced pressure (~ 100 mbar). Because of the difference in partial pressure, hydrogen dissolved in liquid comes out of solution, leading to pores approximately ten times larger in size than in atmospheric pressure. The sample is then cut in half, and the appearance of the sample cross section is interpreted regarding the quality of the melt. Hence, reduced pressure test remains an inexpensive test that yields quick results.

Although reduced pressure test has been available for several decades, metrics that can be used based on the test

results have not been widely used in industry. The present study is motivated by the gap in the literature where metrics from reduced pressure test data is used to assess aluminium melt quality. To accomplish this, various melt treatments, including degassing, Si modification additions, grain refining additions, were applied to A356 alloy melts and metallographic data were collected and interpreted.

Background

Pores in aluminum castings have been attributed¹¹ to shrinkage of metal during solidification and to the significant drop of solubility of hydrogen during phase change from liquid to solid.¹² Hydrogen is thought to segregate in front of the dendrites and transform to gas phase due to low solubility and form porosity. Thus, the measurement of the hydrogen content of the melt prior to casting has preoccupied foundry engineers. However, it has been demonstrated that (1) it is impossible for pores to nucleate in liquid aluminum either homogeneously or heterogeneously,^{13,14} and (2) the equilibrium vacancy concentration in aluminum at the melting temperature is sufficient to accommodate the excess hydrogen.¹³ The only mechanism for pore formation is the entrainment of surface oxides to form bifilms,^{11,15} which open up during solidification under negative pressure and/or segregation of hydrogen during solidification. Under reduced pressure, the air between the folded oxide layers is expanded and the bifilms are unraveled.¹⁶ While this process is easier for young bifilms which have formed during mold filling, for coarse “old” oxides from ingot surface or crucible, this may be harder. Therefore, observation of round pores in the cross section of RPT samples indicates young oxides (amorphous and thin) and crack-like pores usually show the presence of old oxides (thick and more rigid).

The quantification of RPT results in assessing the melt quality was attempted by several researchers. LaOrchan et al.¹⁷ used four different Al–Si alloys, and a constant volume sample allows to estimate the hydrogen concentration by weighing of the sample upon solidification. It was shown that there was an inverse relationship between hydrogen level and the weight of the specimen. Dasgupta et al.¹⁸ investigated to correlate reduced pressure test results and hydrogen content of the melt and claimed that there was a correlation of RPT densities with AlScan hydrogen values for a given alloy. Hence, it was possible to estimate the hydrogen content in the melt from the density

of an RPT sample. They also published a curve to show the relationship between hydrogen content (cc/100 g) and temperature (°C). Dispinar and Campbell¹⁹ compared the results from existing methods to assess melt quality and stated that there was no direct correlation between hydrogen content and porosity in cast aluminum alloys.

A metric that can be used to quantify the melt quality based on RPT results was introduced by Dispinar and Campbell^{19–23} to monitor both inclusions (bifilms) and hydrogen content together after digital image analysis of the cross section of the RPT sample. They proposed to measure the maximum length of pores as an indication of bifilm length and introduced a new metric, called the bifilm index, B_I :

$$B_I = \sum (\text{pore length}) \quad \text{Eqn. 1}$$

Subsequently, the effect of bifilm index on the quality of the final casting was investigated,^{15,24–29} as measured by tensile properties. In general, when the bifilm index decreased (better melt quality), tensile strength and elongation increased. However, this result did not apply to every casting, because bifilms were not homogeneously distributed within the melts. Their size, shape and number also varied from one melt to another. Therefore, an important aspect of RPT is the quantification of distribution of bifilms within the entire melt. Hence, several samples need to be collected from the same melt because measured bifilm index values have a certain degree of variation,²² as evidenced by large error bars and scatter of bifilm index measurements. Because bifilm index combines the size and the number density of the pores on RPT into a single metric, it is not well understood whether this variability is consistent or not. Therefore, it is not clear whether the sources of variation are the size or number of bifilms. Moreover, the physical meaning of bifilm index has not been well established. To address these issues, the quality of A356 alloy melts under six conditions with various modification additions, with and without degassing, has been assessed via RPT. The results have been analyzed statistically.

Experimental Works

A356 ingots used in the study, with the chemical composition given in Table 1, were provided by ETI ALUMINIUM, Turkey. Ingots were melted in a SiC crucible in an electric furnace with a capacity of 20 kg. AlTi5B1 and

Table 1. Chemical Composition of A356

Alloy	Si	Fe	Cu	Mn	Mg	Zn	Ti	Al
A356	6.80	0.19	0.003	0.001	0.30	0.011	0.108	Rem.

Table 2. Chemical Composition of Master Alloys

Master alloys	Ti	Sr	B	Fe	Si	Ca	Al
AlSr15	–	% 14–15	–	≤ % 0.2	≤ % 0.2	≤ % 0.2	Rem.
AlTi5B1	% 5	–	% 1	≤ % 0.2	≤ % 0.2	–	Rem.
Al3B	–	–	% 2.5–3.5	% 0.3	% 0.2	–	Rem.

Table 3. Experimental Parameters

Number	Parameters
1	No addition – (no degassing)
2	No addition – degassed
3	AlSr15 – (no degassing)
4	AlSr15 + degassed
5	AlSr15 and AlTi5B1 – (no degassing)
6	AlSr15 and AlTi5B1 + degassed
7	AlTi5B1 – (no degassing)
8	AlTi5B1 + degassed
9	Al3B – (no degassing)
10	Al3B + degassed
11	AlSr15 and Al3B – (no degassing)
12	AlSr15 and Al3B + degassed

Al3B were added for grain refinement, and AlSr15 was added for Si modification when the temperature of the melt was at 740 °C. Chemical compositions of the AlTi5B1, Al3B and AlSr15 that were used in this study are given in Table 2. Ti and B concentration was selected to be 10 ppm. A concentration of 30 ppm was used for Sr modification. Experimental details of this study are summarized in Table 3.

Experimental work was carried out under two conditions: degassed and non-degassed. A T-type graphite lance was used for degassing at 740 °C. Degassing duration was selected to be 20 min with 2 L/min flow rate. Argon was preferred for degassing process. After degassing process, grain refinement and/or modification alloys were added into the liquid metal and surface of the liquid was skimmed prior to casting. More details about the experiments are given elsewhere.³⁰

RPT samples were poured in a sand mold and solidified under a pressure of 80 mbar. Two samples that have a rectangular shape with 55 mm height and 10 mm thickness were produced. Samples were cut into two, and cross section was grinded. A total of 120 RPT samples were produced. A scanner was used to capture images of the surface of RPT samples with high resolution. SigmaScan image analysis software was used to obtain pore size and number data, which were later used to calculate melt quality metrics, including bifilm index. Data obtained from

these RPT samples were statistically analyzed, i.e., the distribution of number density (N), the total diameter of pores ($N\bar{d}$), the total area of pores ($N\pi\bar{d}^2/4$), the total volumes of pores ($N\pi\bar{d}^3/6$). Finally, relationships between bifilm index and % bifilm area, N , $N\bar{d}$, $N\pi\bar{d}^2/4$, $N\pi\bar{d}^3/6$, were determined.

Results and Discussion

Cross sections of some representative RPT samples are given in Figure 1. At first glance, the differences between no degassing and degassed conditions are evident. The degassing process plays an important role to decrease bifilms.^{30–32} It is an interesting point that grain refiners decreased bifilms without degassing. RPT images of AlTi5B1 and Al3B additions without degassing have bifilms less than images of the other addition parameters. Degassed melts of AlTi5B1, Al3B and AlSr15 + AlTi5B additions have lower bifilm content than the other parameters.

Statistical analysis was carried out from all pore size measurements. Subsequently, it was hypothesized that d_{eq} followed the lognormal distribution, which is consistent with the theory that pore size distribution in castings should be lognormal³³ as well as observations in Mg³⁴ and Al³⁵ alloy castings. The density function (f) for the lognormal distribution is written as;

$$f(d_{eq}) = \frac{1}{d_{eq}\sigma\sqrt{2\pi}} \exp\left[-\frac{(\ln(d_{eq}) - \mu)^2}{2\sigma^2}\right] \quad \text{Eqn. 2}$$

where σ is the shape and μ is the scale parameter. The expected value, i.e., mean of a lognormal distribution, is found by;

$$\bar{d}_{eq} = e^{\mu + \sigma^2/2} \quad \text{Eqn. 3}$$

Parameters of the lognormal distribution were estimated by using the maximum likelihood method. The goodness of fit of the estimated parameters was tested by using the Anderson–Darling statistic.³⁶ In all cases, the hypothesis that the data come from the fitted lognormal distributions could not be rejected. The results of the lognormal distribution of pore diameter from RPT samples for three of twelve parameters are given in Figure 2. It can be seen that when AlSr15 and AlTi5B1 added into the melt together, average pore diameter becomes minimum. This value is maximum for the as-received condition. The

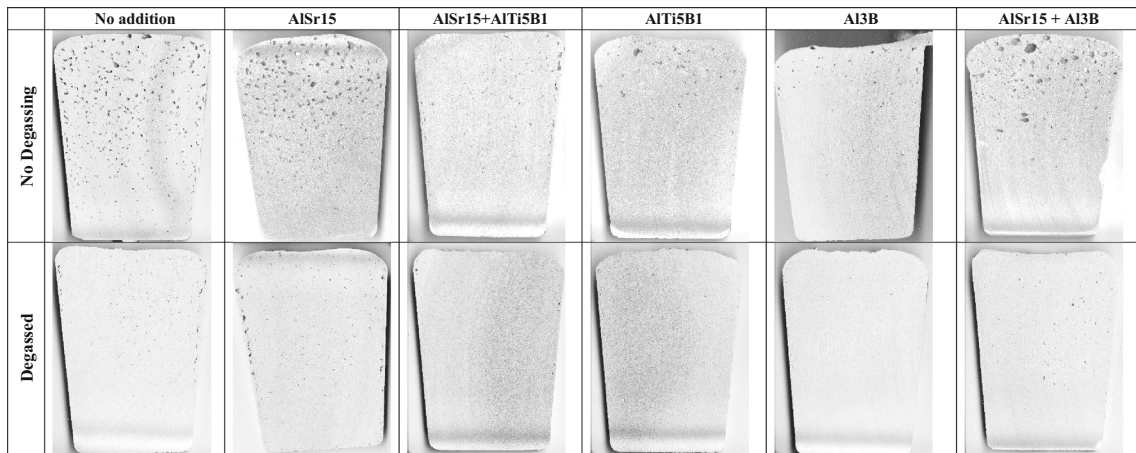


Figure 1. Representative RPT images for experimental studies.

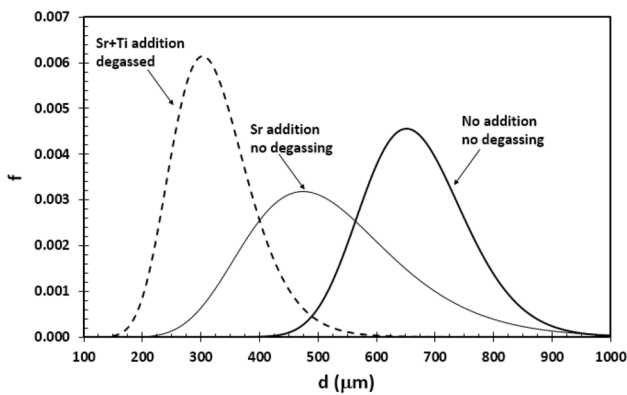


Figure 2. Lognormal distributions of pore diameter from RPT samples for three parameters of experiment.

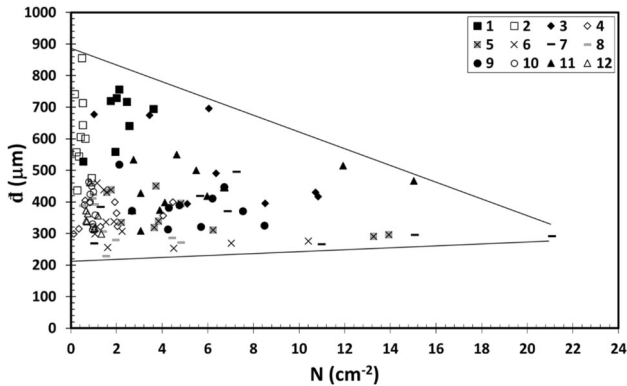


Figure 3. The relationship between number density (N) and average diameter (\bar{d}) of pores.

addition of AlSr15 decreased the average diameter. As the melt is degassed, the distribution of pore sizes becomes narrower and steeper.

The number density of pores was calculated on all the samples, and the relationship between number density and equivalent diameter of pores was investigated. The result of these findings is given in Figure 3, which shows a strong

relationship between number density and the average diameter of pores. As the number density of pores goes up, the average diameter of pores tends to get smaller. In other words, there is an inverse relationship between them. Yet, there appears to be a lower boundary where average diameter of pores remains essentially constant, as indicated by the lower line.

A possible correlation between number density of pores on RPT samples and bifilm index was also evaluated. Figure 4 shows that the relationship between number density and bifilm index is poor. However, it can be concluded from the graph that melt treatments have a different effect. Each parameter seems to have an exponential lookalike but close to linear relationship on its own.

The relationship between total diameter and bifilm index was investigated. The total diameter was calculated taking into account number density and average diameter together. These results are given in Figure 5. Compared to Figure 4, there appears to be linearity between total area and bifilm index at different slopes for each different parameters, but not sufficient to extract the meaning of the bifilm index in general terms.

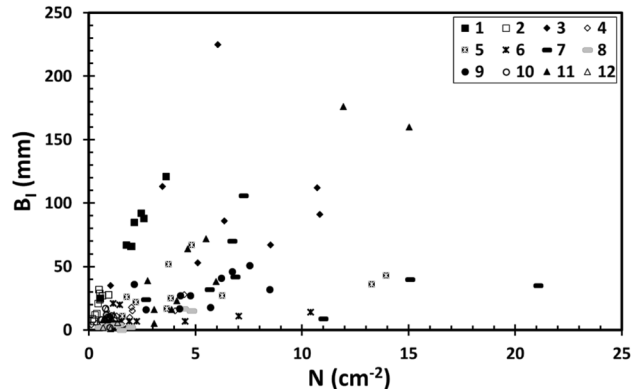


Figure 4. Bifilm index (B_i) versus number density (N).

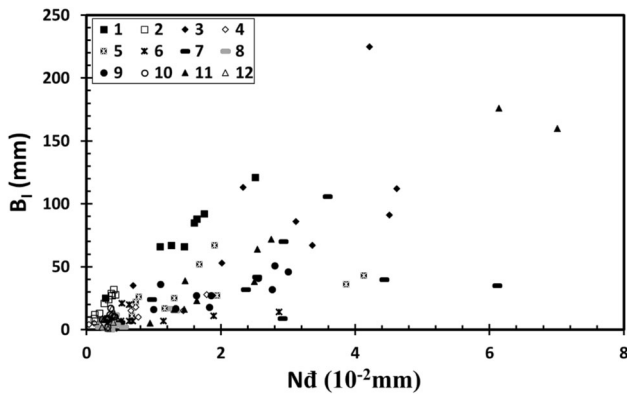


Figure 5. Bifilm index (B_i) versus $N\bar{d}$.

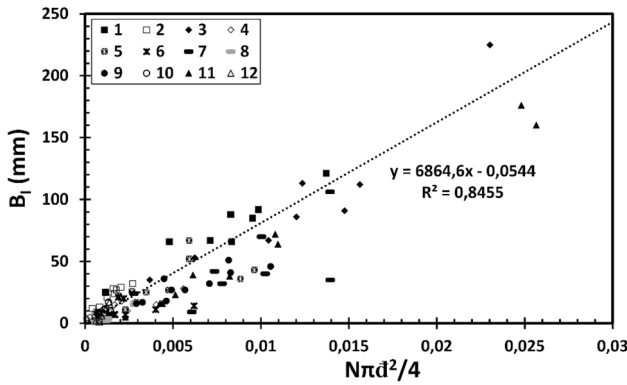


Figure 6. Bifilm index (B_i) versus $N\pi\bar{d}^2/4$.

The relationship between bifilm index and the total area of pores, as calculated by the product of number density and the area of the average pore, is presented in Figure 6, which shows that the relationship is linear with an R^2 value of 0.846. It can be concluded that the relationship between the total area of pores and bifilm index is better than the relationship between the total diameter of pores and bifilm index. Alternatively, the area of pores on the surfaces of RPT samples was calculated and the results are given in Figure 7. This relationship has an R^2 value of 0.781 which is lower than the previous relationship.

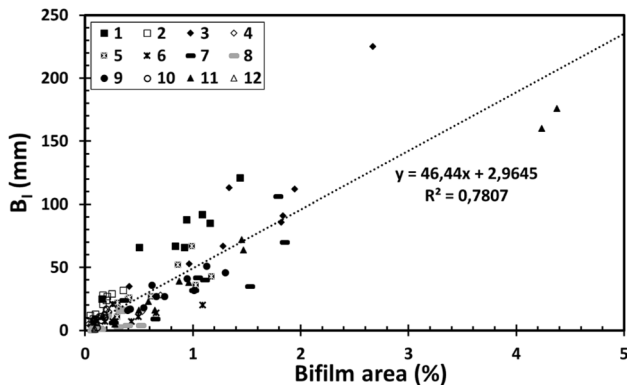


Figure 7. Bifilm index (B_i) versus bifilm area %.

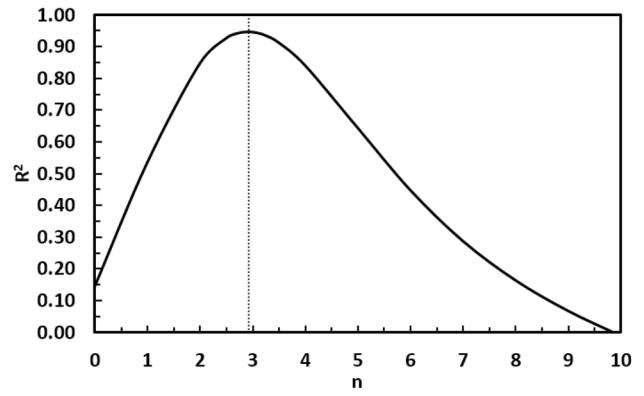


Figure 8. Optimum n value for R^2 .

The search for the meaning of bifilm index was continued by extracting the following formulation: $N d^n$, where N is the number density of pores, d is the average diameter of pores, and n is the exponent. The n value for maximum R^2 was calculated to be 2.92, as indicated in Figure 8. Because of its proximity, n was chosen as 3 for the next step of analysis to investigate the meaning of the bifilm index. The total volume of pores was calculated as the product of number density of pores and $\pi d^3/6$. The relationship between the total volume of pores and bifilm index is given in Figure 9. The result shows that there is a strong relationship between bifilm index and volume of pores, as evidenced by an R^2 of 0.9495. This shows that if all the pores were perfectly spherical, a linear relationship between the volume of pores and bifilm index could be expected with $R^2 = 1.0$.

One of the interesting findings of this study was found when all the graphs in Figures 4, 5, 6, 7, 8 and 9 are plotted again where the maximum value of bifilm index was taken as 50 mm. As shown in Figure 10, for bifilm index values above 50 mm, the linearity of the data is high. This means that the volume of pores can be used to define casting quality. It is interesting to note that when bifilm index is over 50 mm, this indicates that the melt quality is quite poor. This raises the question: If the quality is bad, do we really need to measure it? Clearly, if the quality is bad, the

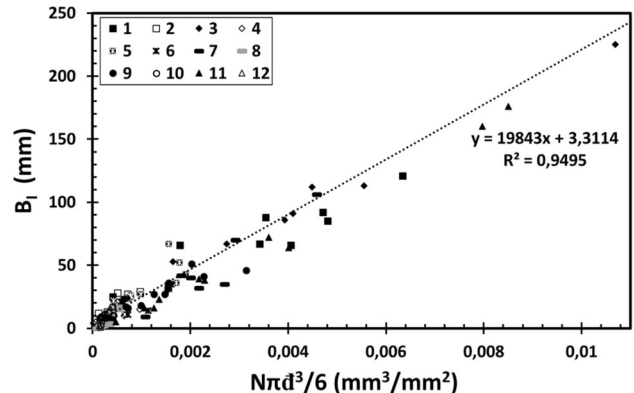


Figure 9. Bifilm index (B_i) versus $N\pi\bar{d}^3/6$.

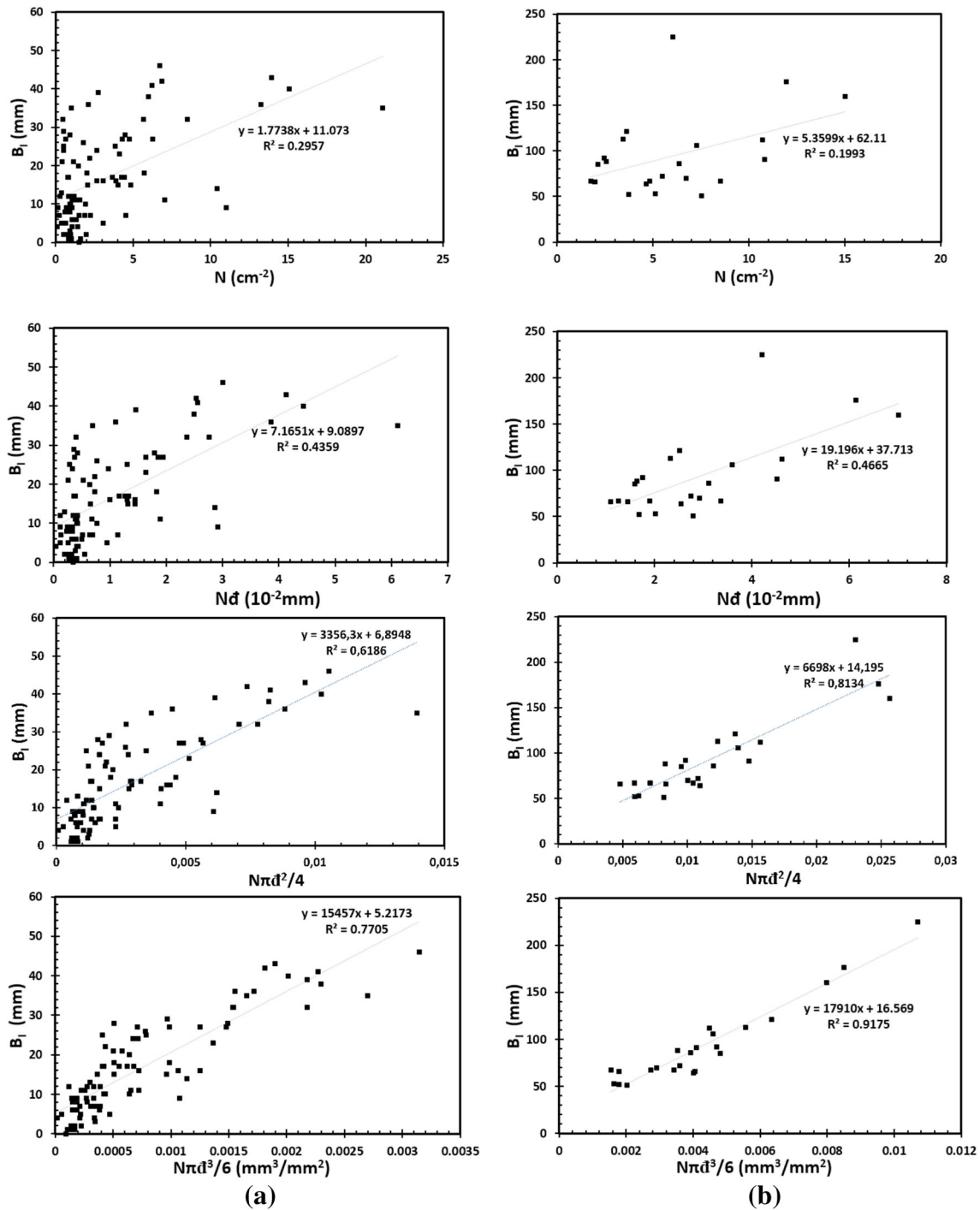


Figure 10. Number density of pores, average pore density and bifilm index change. (a) Bifilm index below 50 mm, (b) bifilm index above 50 mm.

melt needs to be further processed to achieve higher quality. When bifilm index is below 50 mm, the correlation between total volume of pores and the bifilm index becomes less strong. The reasons for an increased scatter with increasing melt quality are not clear. It is the authors' opinion that the bifilm index be used as a guide for higher-quality melts, with the following scales:

- $0 \leq B_I \leq 10$ mm: high-quality melt

- $10 \leq B_I \leq 25$ mm: good quality
- $25 \leq B_I \leq 50$ mm: average quality
- $50 \leq B_I \leq 100$: unacceptable quality
- $B_I \geq 100$: bad quality that should be avoided

In general terms, the base alloy in its as-received state has the highest bifilm index with a low number of pore density. As the alloy is Sr modified, number density of pores increases with lowered bifilm index followed by Ti and B

additions (i.e., grain refiners) which suggests that as Si is modified and grains get smaller, bifilm index decreases, but the number of pores increases. Once the melt is degassed, melt quality is increased by 60%.

Conclusions

- There is a relationship between number density of pores and the average diameter of pores. As the number density of pores increases, the average diameter of pores is reduced.
- There is no relationship between number density of pores, total diameter of pores and bifilm index. However, there is a good relationship between the total volume of pores and bifilm index, only when bifilm index is higher than 50 mm. On the other hand, for accurate quantification of A356 melt cleanliness, bifilm index needs to be used.
- The ideal way to produce defect-free castings, a melt with zero bifilm index has to be achieved. When working with the A356 alloy, 50-mm bifilm index is the upper limit for good-quality castings.
- Degassing is an effective process to decrease pore formation in A356 alloy by simply removing bifilms from the melt. Al-Sr master additions decrease bifilm index (i.e., improves melt quality) but increase the number of pore density suggesting the distribution of bifilms along the cast part. Al5Ti1B and/or Al3B grain refiner addition further decreases bifilm index and further distributes pores. In general, master alloys and grain refiners affect the average diameter of pores to become smaller and homogeneously distributed.

Acknowledgements

This work has been supported by the Scientific Research Projects Coordination Unit of Selcuk University (Project Number: 13101026). The author would like to thank TUBITAK (Turkey) for its support.

REFERENCES

1. C. Ransley, D. Talbot, The routine determination of the hydrogen content of aluminium and aluminium alloys by the hot-extraction method. *J. Inst. Met.* **84**, 445–452 (1956)
2. C. Ransley, D. Talbot, H. Barlow, An instrument for measuring the gas content of aluminum alloys during melting and casting. *J. Inst. Met.* **58**, 86 (1957)
3. D. Neil, A. Burr, Initial bubble test for determination of hydrogen content in molten aluminum. *AFS Trans.* **69**, 272–275 (1961)
4. G. Grigorenko, V. Lakomskii, D. Rabkin, Determination of the amount of hydrogen in aluminum and aluminum alloys containing components with low vapor pressures. in *Gases in Cast Metals* (1965), p. 247
5. J. Church, K. Herrick, Quantitative gas testing for production control of aluminum casting soundness. *AFS Trans.* **78**, 277–280 (1970)
6. X.-G. Chen, S. Engler, Measuring hydrogen content in molten aluminium alloys using the CHAPEL technique. *Cast Met.* **6**, 99–108 (1993)
7. L. Martins, C. Sanderson, J. Tessandori, NOTORP hydrogen analyzer operating principles and application at commonwealth aluminum. in *Light Metals* (Warrendale, 1998), pp. 817–826
8. Systems, M. *Hyscan*. 2016; Available from: <http://www.mechatechsystems.co.uk/severn-science>
9. ABB. *Alscan*. 2016; Available from: <http://new.abb.com/products/measurement-products/analytical/metallurgical-analyzers/alscan>
10. Foseco. *Alspek*. 2016; Available from: http://www.vesuvius.com/fileadmin/_migrated/content_uploads/ALSPEK_H_e__03.pdf
11. J. Campbell, *Complete Casting Handbook: Metal Casting Processes, Metallurgy, Techniques and Design* (Butterworth-Heinemann, Oxford, 2015)
12. C. Ransley, H. Neufeld, The solubility of hydrogen in liquid and solid aluminium. *J. Inst. Met.* **74**(12), 599–620 (1948)
13. P. Yousefian, M. Tiryakioğlu, Pore formation during solidification of aluminum: reconciliation of experimental observations, modeling assumptions, and classical nucleation theory. *Metall. Mater. Trans. A* **49**(2), 563–575 (2018)
14. J. Campbell (1968) *Pore Nucleation in Solidifying Metals. The Solidification of metals: proceedings of the conference on The solidification of Metals*, 1968: p. 18–26
15. J. Campbell, Entrainment defects. *Mater. Sci. Technol.* **22**(2), 127–145 (2006)
16. S. Fox, J. Campbell, Visualisation of oxide film defects during solidification of aluminium alloys. *Scripta Mater.* **43**(10), 881–886 (2000)
17. W. LaOrchan, M. Mulazimoglu, X. Chen, J. Gruzleski, Quantified reduced pressure test. *Trans. Am. Foundrymen's Soc.* **103**, 565–574 (1995)
18. B. DasGupta, L. Parmenter, D. Apelian. Relationship between the reduced pressure test and hydrogen content of the melt. in *Proceedings, 5th International Conference on Molten Metal Processing, AFS, Orlando* (1998)
19. D. Dispinar, J. Campbell, Use of bifilm index as an assessment of liquid metal quality. *Int. J. Cast Met. Res.* **19**(1), 5–17 (2006)
20. D. Dispinar, J. Campbell, Critical Assessment of Reduced Pressure Test. Part 2: quantification. *Int. J. Cast Met. Res.* **17**(5), 287–294 (2004)

21. D. Dispınar, J. Campbell, Critical assessment of reduced pressure test. Part 1: porosity phenomena. *Int. J. Cast Met. Res.* **17**(5), 280–286 (2004)
22. D. Dispınar, J. Campbell, Porosity, hydrogen and bifilm content in Al alloy castings. *Mater. Sci. Eng., A* **528**(10–11), 3860–3865 (2011)
23. D. Dispınar, J. Campbell. *Reduced Pressure Test (RPT) For Bifilm Assessment.* in *143rd TMS Annual Meeting, 5th Shape Casting.*, 2014. San Diego, USA
24. G.E. Bozchaloei, N. Varahram, P. Davami, S.K. Kim, Effect of oxide bifilms on the mechanical properties of cast Al–7Si–0.3 Mg alloy and the roll of runner height after filter on their formation. *Mater. Sci. Eng., A* **548**, 99–105 (2012)
25. J. Campbell, An overview of the effects of bifilms on the structure and properties of cast alloys. *Metall. Mater. Trans. B* **37**(6), 857–863 (2006)
26. J. Campbell, Stop pouring, start casting. *Int. J. Metalcasting* **6**(3), 7–18 (2012)
27. M.A. El-Sayed, H.A. Salem, A.Y. Kandeil, W. Griffiths, Effect of holding time before solidification on double-oxide film defects and mechanical properties of aluminum alloys. *Metall. Mater. Trans. B* **42**(6), 1104–1109 (2011)
28. B. Farhoodi, R. Raiszadeh, M.-H. Ghanaatian, Role of double oxide film defects in the formation of gas porosity in commercial purity and Sr-containing Al alloys. *J. Mater. Sci. Technol.* **30**(2), 154–162 (2014)
29. K. Haberl, P. Schumacher, G. Geier, B. Stauder, Characterization of the melt quality and impurity content of an LM25 alloy. *Metall. Mater. Trans. B* **40**(6), 812 (2009)
30. M. Uludağ, R. Çetin, D. Dispınar, M. Tiryakiođlu, Characterization of the effect of melt treatments on melt quality in Al-7wt %Si-Mg alloys. *Metals* **7**(5), 157 (2017)
31. D. Dispınar, A. Nordmark, M. Di Sabatino, S. Akhtar, L. Arnberg, Degassing, hydrogen and porosity phenomena in A356. *Mater. Sci. Eng., A* **527**(16–17), 3719–3725 (2010)
32. Yorulmaz, A., Ç. Yüksel, E. Erzi, and D. Dispınar. *Effects of Casting Conditions on End Product Defects in Direct Chill Casted Hot Rolling Ingots.* in *Shape Casting: 6th International Symposium.* 2016. Springer
33. H. Dvorak, E. Schwegtier, Statistical distribution of flaw sizes. *Int. J. Fract. Mech.* **8**(1), 110–111 (1972)
34. M. Tiryakiođlu, Pore size distributions in AM50 Mg alloy die castings. *Mater. Sci. Eng., A* **465**(1), 287–289 (2007)
35. M. Tiryakiođlu, On fatigue life variability in cast Al–10% Si–Mg alloys. *Mater. Sci. Eng., A* **527**(6), 1560–1564 (2010)
36. T.W. Anderson, D.A. Darling, A test of goodness of fit. *J. Am. Stat. Assoc.* **49**(268), 765–769 (1954)